# Numerical Investigation of Air-Coupled Generation of Lamb Waves in Isotropic Plates

A. Vilpisauskas[1], R. Kazys[1]
[1]*Ultrasound Institute, Kaunas University of Technology,*
*Studentu St. 50, LT-51368 Kaunas, Lithuania*
*almvilp@gmail.com*

***Abstract*—In the case of non-destructive testing and evaluation (NDT & NDE) of plate materials and structures ultrasonic Lamb waves are used. Very often air-coupled ultrasonic transducers are used for non-contact Lamb wave excitation and reception. This method has a very serious drawback: global insertion losses for an air-coupled system may be 120 dB–160 dB typically. In order to improve this NDT method a better understanding of Lamb wave excitation process is needed. A numerical investigation was performed in order to evaluate air-coupled Lamb wave excitation in an isotropic single layer plate. It is shown how Lamb wave normal displacement amplitude depends on an incidence angle and the distance between the plate and the transducer.**

***Index Terms*—Air-coupled ultrasonic, isotropic single layer plate, Lamb waves, numerical simulation.**

## I. INTRODUCTION

Many ultrasonic NDT methods use couplants between the material under a test and ultrasonic transducers. However there are certain cases where this is not possible, because the tested material may be damaged or contaminated by a couplant, for example paper, wooden, aerospace and composite materials.

It is not a new idea in NDT to use non-contactly without couplant generated Lamb waves (or guided waves) for testing of plate materials. Different techniques are used, for example lasers [1], [2], EMATs (Electro-Magnetic Acoustic Transducers) [3], electrostatic excitation methods [2]. Air-coupled generation of Lamb waves in plate materials is becoming the most popular method in NDT [4]–[13]. Popularity of this method still grows up. There is a demand on improvements, and numerical model of entire Lamb wave system is needed. Usually Finite Element Method (FEM) based models are used to calculate Lamb wave propagation in plate structures and Impulse Response Method (IRM) based models are used to calculate acoustic pressure, radiated by air-coupled transducer [12], [13]. Those hybrid models are exact enough, but they still require a lot of computational time and storage for output data.

Reference [14] shows that in the case of an isotropic single layer plate entire air-coupled Lamb wave system can be modelled analytically. For this purpose the free software tool "The Lamb Matlab toolbox" (Beta version 0.1) was written [15].

Manuscript received February 28, 2013; accepted July 9, 2013.

The objective of this research was to investigate Lamb wave amplitude dependency on the incidence angle and signal frequency at the different distances between the plate and the emitting transducer, corresponding to transducer pressure signal near field, intermediate field and far field zones.

## II. NUMERICAL SIMULATION METHODS

The acoustic pressure, generated by a rectangular piston in liquid or gas type medium, is calculated using the Impulse Response Method (IRM) [16]–[18].

Let us consider a rectangular transducer 2*b* long and 2*a* ($a \le b$) wide and located in $z = xy0$ plane (Fig. 1(a)).

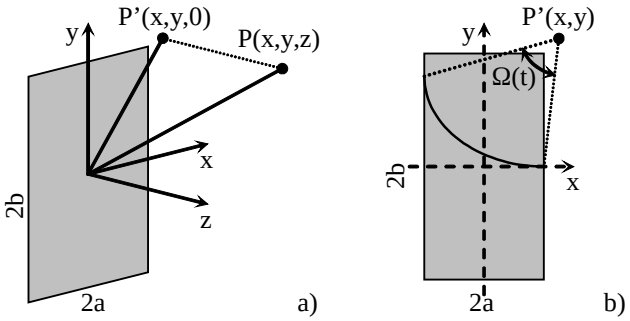


Fig. 1. Geometry and coordinate system for calculation of the impulse response of a rectangular transducer.

The impulse response function *h* depends on time *t*, spatial coordinates of the point *P(x,y,z)*, where this function is calculated, the sound velocity *c* in a medium, the obliquity factor *β(z,t)* corresponding to the transducer boundary conditions and the angle *Ω(P',t)*, subtended at the point *P'* (Fig. 1(b)) by the arc (1)

$$h(P,t) = c \cdot \frac{(z,t)}{4®} \cdot \Omega(P',t). \qquad (1)$$

The obliquity factors *β(z,t)* are given in the time domain (2)

$$(z,t) = \begin{cases} 2, & \textit{rigid baffle}, \\ 2z/(ct), & \textit{soft baffle}, \\ 1+[z/ct], & \textit{free field}. \end{cases} \qquad (2)$$

When the transducer vibrates at the velocity *v(t)* in a liquid or gas type medium with the density *ρ*, then the

transient pressure $p(P,t)$ in the point $P(x,y,z)$ is calculated using convolution operation (*) (3)

$$p(P,t) = \circ \frac{\partial v(t)}{\partial t} * h(P,t), \quad (3)$$

In the case of air-coupled transducers the distance dependent attenuation should be estimated. This is done by calculating the attenuated impulse response function $h_a(P,t)$, when the inverse Fourier transform is applied to the calculated impulse response function in the frequency domain $H(i\omega)$, multiplied by the attenuation function $A_{atte}(P,i\omega)$ (4)

$$h_a(P,t) = \frac{1}{2®} \int_{-\infty}^{+\infty} A_{atte}(P,i\mu) H(i\mu) d\mu. \quad (4)$$

For the calculation of the air attenuation see [14], [19].

If an infinite isotropic plate is excited by a time harmonic signal, which exerts pressure over a finite radius circular region, then normal displacements in the plate can be calculated using the Time Harmonic Solution (THS) method [14], [20]. Because of the THS method complexity we shall not analyze it in more detail. We mention that the explained solution assumes the Continuous Wave (CW) is used. For the transient signal a finite set of harmonic excitation frequencies are used, and normal displacements are obtained by using a harmonic summation method.

In "The Lamb Matlab toolbox" software tool finite excitation zone is divided into circular sub-regions of radius $a$. The pressure signal is calculated at the center point of a circular sub-region and taken equal in all sub-region area. The radius $a$ should be small, at least four times smaller than the minimum Lamb wavelength. Total normal displacement signal at the given plate point is computed by superposition of normal displacements, created by all circular sub-regions.

## III. NUMERICAL INVESTIGATION

Numerical investigation was performed simulating air-coupled Lamb wave excitation in an aluminium plate of 2 mm thickness, and 2D approach was used (Fig. 2). "The Lamb Matlab toolbox" software tool was checked, corrections were made in excitation signal generation, transducer geometry calculation, excitation and emission zone coordinate points calculation. New set of functions was written for emitting transducer generated pressure signal visualization. Missing code for the obliquity factors "soft baffle" and "free field" was written newly.

The square air-coupled transducer $T$ has dimensions 15 mm × 15 mm, it is located at the distance $R$ from the excitation zone centre on the plate surface and deflected by the incidence angle $\alpha$. The length of x-line type excitation zone is set to $L_{EZ}$ = 70 mm, the zone is filled with 176 circular excitation sub-regions of the $a$ = 0.2 mm radius. The normal displacement signal is calculated at the point $P$, situated on the plate's surface at $x_0$ = 50 mm distance from the excitation zone centre.

The rigid baffle obliquity factor $\beta(z,t)$ = 2 was used in transducer $T$ simulations. The transducer $T$ surface radiates a narrow-band particle velocity signal of 20 cycles sinus pulse with the sinus type envelope, 1 m/s amplitude and 100 MHz sampling frequency. Two different frequencies were used: 150 kHz with the 50 kHz–500 kHz limited bandwidth and 260 μs THS time limit (Fig. 3); 500 kHz with the 300 kHz–900 kHz limited bandwidth and 180 μs THS time limit.

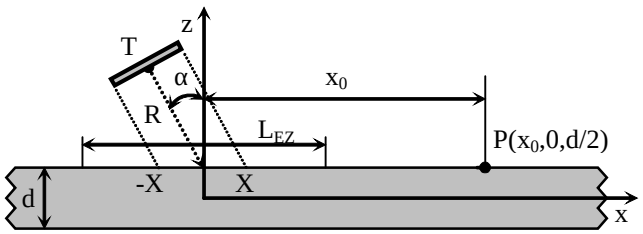


Fig. 2. Schematic diagram of air-coupled Lamb wave excitation in plate.

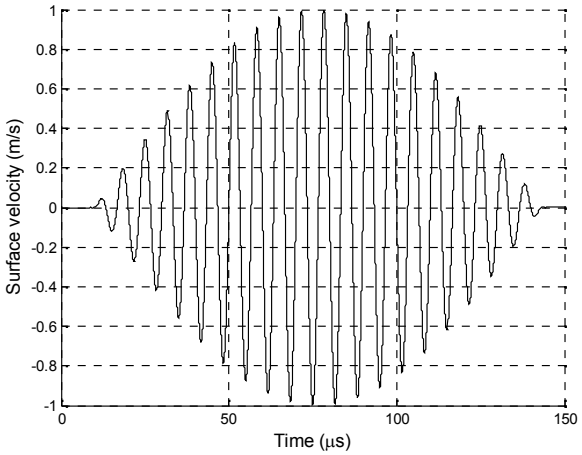


Fig. 3. Transducer $T$ velocity signal: main frequency 150 kHz, limited in (50-500) kHz frequency bandwidth.

The structure of transducer pressure field changes along the distance $R$. Three zones exist: near field, intermediate field and far field, so Lamb wave excitation conditions are different. The transducer's $T$ near field limit $NFL$ is calculated as (5) [21]

$$NFL = 1.37 \frac{a^2}{\lambda}, \quad (5)$$

where $a$ is the length of the square transducer side; $\lambda$ is the sound wavelength in air. For 150 kHz frequency $NFL_{150}$ = 33.68 mm, and for 500 kHz frequency $NFL_{500}$ = 112.34 mm. According to the 150 kHz frequency near field limit, three distances $R$ were chosen: $R$ = 10 mm for a near field; $R$ = 35 mm for intermediate field (when transducer is deflected, one part of the excitation zone gets into the near field, and the other – in the far field pressure zone), $R$ = 45 mm for far field. The pressure signal, generated in the excitation zone at $R$ = 10 mm distance and $\alpha$ = 0° incidence angle, is shown in Fig. 4. Transducer's $T$ deflection angle $\alpha$ was changed from 0° to 30° using step of 0.5°. The normal displacement signal of the $A_0$ Lamb wave mode was calculated at the point $P$. The value of maximum positive peak amplitude is taken; dependencies versus deflection angle $\alpha$ and the distance $R$ were plotted (Fig. 5–Fig. 6).

The experimental dependency (Fig. 7) was obtained using two air coupled transducers. The emitter was deflected with

respect to aluminum plate; the receiver was tuned according to the signal maximum and then fixed. Five peak-to-peak dependencies were obtained, then averaged and normalized. A reasonable degree of similarity between the theory and the experiment was obtained.

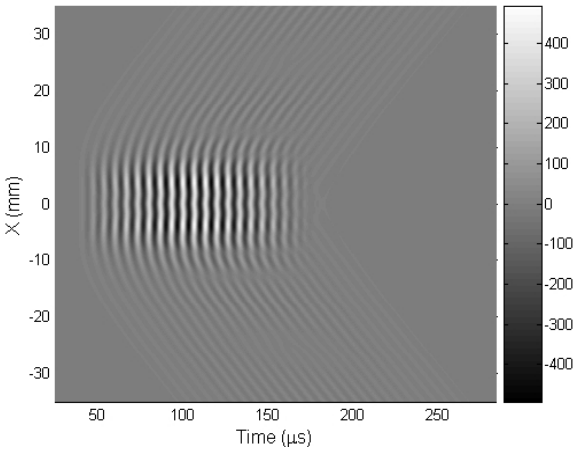


Fig. 4. Typical pressure signal (in Pa), generated in excitation zone at $R$=10 mm distance and $\alpha$=0º incidence angle.

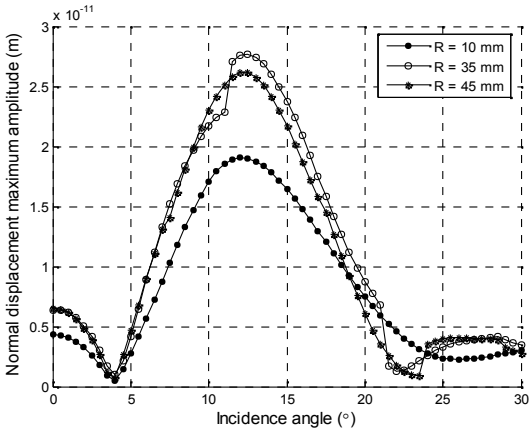


Fig. 5. Dependency of $A_0$ mode normal displacement amplitude maximum positive peak for 2 mm aluminium plate using 150 kHz excitation signal.

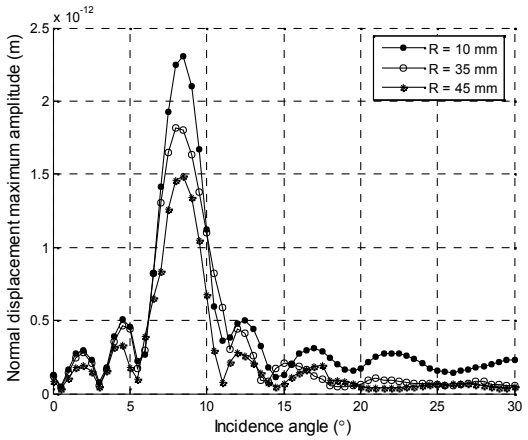


Fig. 6. Dependency of $A_0$ mode normal displacement amplitude maximum positive peak for 2 mm aluminium plate using 500 kHz excitation signal.

The sharp jump in the curve (Fig. 5, $R$ = 35 mm, $\alpha$ = 11º → 11.5º) near the optimum excitation angle has occurred. It was presumed, that jump occurs when pressure signals amplitude and phase spatial characteristics changes in the intermediate field zone. In order to verify presumption, additional simulations were performed for 2 mm aluminium plate using 150 kHz excitation signal. The transducer $T$ was placed at different distances $R$ = 33 mm and $R$ = 37 mm (Fig. 8; curve for $R$ = 35 mm is plotted for comparison). There is no sharp jump near the optimum excitation angle at $R$ = 33 mm, but the sharp jump is obtained at $R$ = 37 mm ($\alpha$ = 13º → 13.5º).

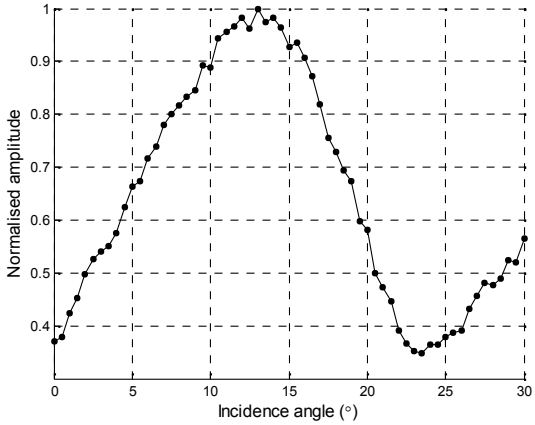


Fig. 7. Experimentally obtained normalised amplitude dependency versus the incidence angle using 150 kHz excitation signal at $R$ = 10 mm.

Different spatial amplitude distributions of pressure fields were estimated by plotting maximum amplitude characteristics versus coordinate $x$. The maximum positive pressure signal value in each of 176 excitation zone signals was detected and graphs were plotted (Fig. 9). It is seen, that the most significant pressure signal values are in the zone below the transducer ($X$ = -7.5 to 7.5 mm).

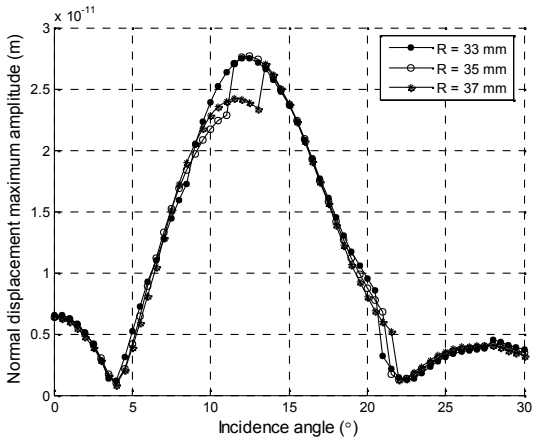


Fig. 8. Dependency of $A_0$ mode normal displacement amplitude maximum positive peak for 2 mm aluminium plate using 150 kHz excitation signal.

Relative time of flight for most of significant pressure signals was estimated as the phase difference between an ideal plane wave front at the optimum incidence angle and the calculated pressure wave front (6)

$$\Delta\varphi(x) = 2\pi f(\tau_\alpha(x) - \tau_{OPT}(x)), \quad (6)$$

where $\Delta\varphi(x)$ is the phase difference at the point $x$; $f$ is the signal frequency; $\tau_\alpha(x)$ is the time of flight of the pressure signal, detected at the 0.25 % relative level; $\tau_{OPT}(x)$ is the time of flight of the pressure signal for the ideal plane wave front at the optimum incidence angle $\alpha_{OPT}$ = 12.7º for 2 mm aluminum plate.

The phase difference characteristics were calculated at

jump points ($R$ = 35 mm, $\alpha$ = 11º → 11.5º; $R$ = 37 mm, $\alpha$ = 13º → 13.5º) (Fig. 10).

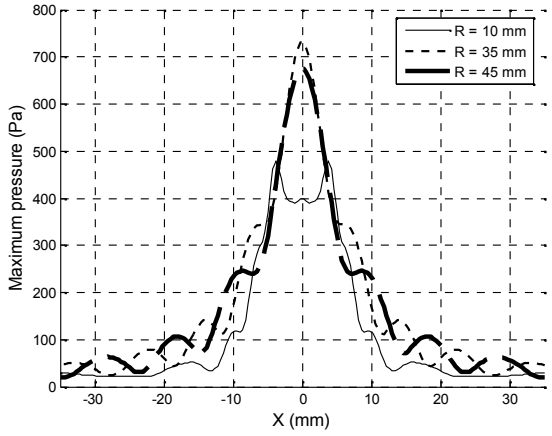


Fig. 9. Maximum pressure value distribution along x-line excitation zone at $\alpha$ = 0º incidence angle.

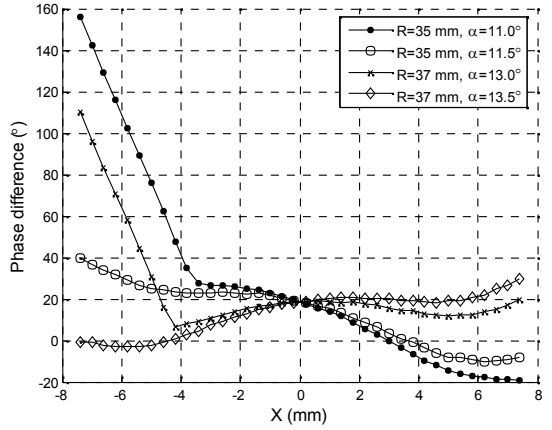


Fig. 10. Pressure signals phase difference characteristics at jump points in normal displacement amplitude maximum positive peak dependency curves.

It is seen in Fig. 10, that before the mentioned jump the phase difference begins to grow up sharply in that part of the excitation zone, where the transducer $T$ is closer to the plate. After the jump the phase difference decreases significantly.

## IV. CONCLUSIONS

It was shown how $A_0$ Lamb wave mode normal displacement maximum amplitude depends on the ultrasonic wave incidence angle and the signal frequency. Different curves were obtained when the distance between the plate and the transducer corresponds to the transducer near field, intermediate field and far field zones. When the excitation zone on the plate surface gets into the transducer intermediate field zone, a jump in the curve near the optimum incidence angle is obtained. The jump is caused by significant phase variations of the incident ultrasonic wave on the plate surface. In the part of excitation zone, where the transducer $T$ is closer to plate, the phase difference has a very sharp, rising character before the jump, and monotonous character after the jump.

## REFERENCES

[1] D. Kim, Y. Cho, J. Lee, "Assesment of wall-thinning in carbon steel pipe by using laser-generated guided wave", *Nuclear engineering and technology*, vol. 42, no. 5, pp. 546–551, Oct. 2010.

[2] Y. Wu, M. de Labachelerie, F. Bastien, "Investigations on excitation and detection methods for Lamb wave sensors", *Sensors and Actuators A*, vol. 100, pp. 214–222, 2002. [Online]. Available: http://dx.doi.org/10.1016/S0924-4247(02)00134-6

[3] R. M. G. Ferrari, "The Acoustoelastic effect: EMAT excitation and reception of lamb waves in pre-stressed metal sheets", in *Proc. COMSOL Conf.*, Milan, 2009.

[4] M. Khoury, G. E. Tourtollet, A. Schroder, "Contactless measurement of the elastic Young's modulus of paper by an ultrasonic technique", *Ultrasonics*, vol. 37, pp. 133–139, 1999. [Online]. Available: http://dx.doi.org/10.1016/S0041-624X(98)00049-3

[5] T. Pettersson, J. Anttila, "On the verification of the applicability of the orthotropic plate wave theory to paper", *Ultrasonics*, vol. 39, pp. 617–622, 2002. [Online]. Available: http://dx.doi.org/10.1016/S0041-624X(02)00357-8

[6] M. J. Garcia-Hernandez, J. A. Chavez, Y. Yanez, H. B. Kichou, J. L. Prego-Borges, J. Salazar, A. Turo, F. Montero de Espinosa, "Ultrasonic Lamb wave NDE system using an air coupled concave array transducer", in *2004 IEEE Int. Ultrasonics, Ferroelectrics and Frequency Control Joint 50th Anniversary Conf.*, pp. 1282–1285.

[7] R. Kazys, A. Demcenko, E. Zukauskas, L. Mazeika, "Air-coupled ultrasonic investigation of multi-layered composite materials", *Ultrasonics*, vol. 44, pp. e819–e822, 2006. [Online]. Available: http://dx.doi.org/10.1016/j.ultras.2006.05.112

[8] R. Kazys, A. Demcenko, L. Mazeika, R. Sliteris, E. Zukauskas, "Air-coupled ultrasonic non-destructive testing of aerospace components", *Insight*, vol. 49, no. 4, Apr. 2007. [Online]. Available: http://dx.doi.org/10.1784/insi.2007.49.4.195

[9] M. Garcia-Rodriguez, Y. Yanez, M. Garcia-Hernandez, J. Salazar, A. Turo, J. A. Chavez, "Lamb wave generation with an air-coupled piezoelectric array using square chirp excitation", in *19th Int. Congr. on Acoustic*, Madrid, Sept. 2007.

[10] Y. Yanez, M. Garcia-Rodriguez, M. J. Garcia-Hernandez, J. Salazar, A. Turo, J. A. Chavez, "Lamb wave generation with an air-coupled piezoelectric concave array using square-wave burst excitation", *NDT&E International*, vol. 41, pp. 292–299, 2008. [Online]. Available: http://dx.doi.org/10.1016/j.ndteint.2007.10.011

[11] R. Raisutis, R. Kazys, E. Zukauskas, L. Mazeika, "Ultrasonic air-coupled testing of square-shape CFRP composite rods by means of guided waves", *NDT&E International*, vol. 44, pp. 645–654, 2011. [Online]. Available: http://dx.doi.org/10.1016/j.ndteint.2011.07.001

[12] G. Dobie, A. Spencer, K. Burnham, S. Gareth Pierce, K. Worden, W. Galbraith, G. Hayward, "Simulation of ultrasonic lamb wave generation, propagation and detection for a reconfigurable air coupled scanner", *Ultrasonics*, vol. 51, pp. 258–269, 2011. [Online]. Available: http://dx.doi.org/10.1016/j.ultras.2010.10.004

[13] M. Masmoudi, M. Castaings, "Three-dimensional hybrid model for predicting air-coupled generation of guided waves in composite material plates", *Ultrasonics*, vol. 52, pp. 81–92, 2012. [Online]. Available: http://dx.doi.org/10.1016/j.ultras.2011.06.014

[14] J. L. Prego-Borges, "Lamb: a simulation tool for air-coupled Lamb wave based ultrasonic NDE systems", Ph.D. dissertation, Dept. Elect. Eng., Spain, Polytechnic Univ. of Catalonia, Barcelona, 2010.

[15] J. L. Prego-Borges, "The Lamb Matlab® toolbox", first release, beta version 0.1, 1 Aug. 2010. [Online]. Available: http://www.mathworks.com/matlabcentral/fileexchange/28367-the-lamb-toolbox

[16] R. Reibold, R. Kazys, "Radiation of a rectangular strip-like focussing transducer. Part 1: harmonic excitation", *Ultrasonics*, vol. 30, no. 1, pp. 49–55, 1992. [Online]. Available: http://dx.doi.org/10.1016/0041-624X(92)90032-H

[17] R. Reibold, R. Kazys, "Radiation of a rectangular strip-like focussing transducer. Part 2: transient excitation", *Ultrasonics*, vol. 30, no. 1, pp. 56–59, 1992. [Online]. Available: http://dx.doi.org/10.1016/0041-624X(92)90033-I

[18] J. L. San Emeterio, L. G. Ullate, "Diffraction impulse response of rectangular transducers", *J. Acoust. Soc. Am.*, vol. 92, no. 2, pt. 1, pp. 651–662, Aug. 1992.

[19] G. Benny, G. Hayward, "Beam profile measurements and simulations for ultrasonic transducers operating in air", *J. Acoust. Soc. Am.*, vol. 107, no. 4, pp. 2089–2100, Apr. 2000. [Online]. Available: http://dx.doi.org/10.1121/1.428491

[20] B. N. Pavlakovic, J. L. Rose, "The influence of finite-size sources in acousto-ultrasonics", *NASA Contractor Report 195374*, Aug. 1994.

[21] J. Krautkramer, H. Krautkramer, *Werkstoffprüfung mit Ultraschall*. Berlin: Springer-Verlag, 1986, pp. 95–99. [Online]. Available: http://dx.doi.org/10.1007/978-3-662-10909-0